Consistent Study of Graphene Structures Through the Direct Incorporation of Surface Conductivity

Georgios D. Bouzianas, Nikolaos V. Kantartzis, Traianos V. Yioultsis, and Theodoros D. Tsiboukis
Dept. of Electrical & Computer Engineering, Aristotle University of Thessaloniki, 54124 Thessaloniki, Greece
E-mail: bouzias@yahoo.gr; kant@auth.gr; traianos@auth.gr; tsibukis@auth.gr

***Abstract*—A novel 3-D FDTD formulation for the precise analysis of electromagnetic wave interactions with graphene structures is presented in this paper. The main concept takes into account the surface nature of graphene's conductivity and incorporates it directly into Maxwell's integral equations, avoiding the necessity to discretize the material's transverse dimension via a subcell scheme. So the proposed technique is much easier to implement and combined with existing FDTD codes, as it requires less computational time. Numerical verification involving comparisons with closed-form solutions and the results of existing schemes, exhibits the high accuracy of the method.**

***Index Terms*—Graphene, auxiliary differential equation, FDTD methods, surface conductivity.**

I. Introduction

Since its initial discovery, graphene has attracted a major scientific interest because of its extraordinary physical properties and promising future prospects [1]. The most critical underlying characteristic is that the energy-momentum relationship for electrons is linear at low energies, rather than quadratic. Consequently, electrons behave as massless relativistic particles of high mobility (Dirac fermions) with an energy-independent velocity, making ballistic transport devices a feasible perspective [2]. Actually, it has already found very interesting applications in the areas of modern integrated circuits [3] and optoelectronics [4], while it is anticipated to be utilized in several devices from transformation optics, taking avail of its competence to support the propagation of surface plasmonic waves [5].

In this paper, a new 3-D explicit methodology is introduced for the treatment of graphene's surface conductivity and therefore the modeling of electromagnetic phenomena in graphene arrangements. The key merit of the algorithm is the direct incorporation of the surface conductivity of graphene into Maxwell's integral equations and their finite-difference time-domain (FDTD) counterparts. For the analysis, the intraband term of the conductivity is considered and the surface current is extracted and inserted in the update expressions via an auxiliary differential equation (ADE). So, the need to employ laborious subcell schemes is efficiently overcome and the proposed technique is much simpler as well as faster than existing approaches, as it requires sufficiently less realization requirements. The frequency-dependent formulation is certified by different setups and the results are compared to closed-form solutions and previously published data.

II. Graphene Surface Conductivity Model

The graphene is described by an infinitesimally thin surface conductivity variation, which via the Kubo formula [2], reads

$$\sigma(\omega,\mu_c,\Gamma,T)=\frac{je^2}{\pi\hbar^2(\omega-j2\Gamma)}\int_0^\infty \varepsilon\left[\frac{\partial f_d(\varepsilon)}{\partial\varepsilon}-\frac{\partial f_d(-\varepsilon)}{\partial\varepsilon}\right]d\varepsilon - \frac{je^2(\omega-j2\Gamma)}{\pi\hbar^2}\int_0^\infty \frac{f_d(-\varepsilon)-f_d(\varepsilon)}{(\omega-j2\Gamma)^2-4(\varepsilon/h)^2}d\varepsilon\,, \quad (1)$$

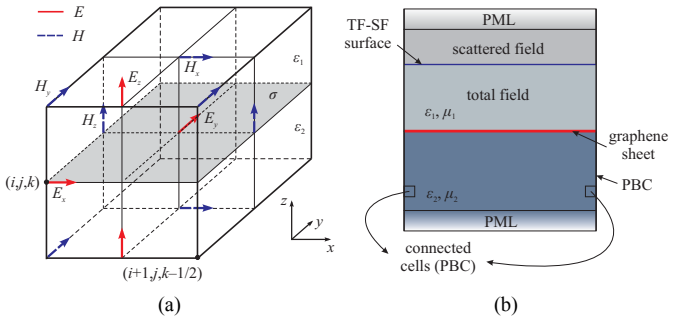

Fig. 1. (a) Modified Yee cell including the graphene surface conductivity and (b) geometry of a graphene arrangement.

with ω the radian frequency, μ_c the chemical potential, Γ a phenomenological scattering rate assumed to be independent of energy ε, T the temperature, $-e$ the electron charge, $\hbar = h/2\pi$ the reduced Planck's constant, $f_d(\varepsilon) = [e^{(\varepsilon-\mu_c)/k_BT}+1]^{-1}$ the Fermi-Dirac distribution, and k_B Boltzmann's constant. Our investigation focuses on the microwave and terahertz frequency spectrum, where the intraband term (first part of (1)) dominates over the interband term (second part of (1)). Furthermore, the chemical potential is obtained in terms of the carrier density n_s,

$$n_s=\frac{2}{\pi\hbar^2v_F^2}\int_0^\infty \varepsilon\left[f_d(\varepsilon)-f_d(\varepsilon+2\mu_c)\right]d\varepsilon\,, \quad (2)$$

where $v_F = 9.5\times10^5$ m/s is the Fermi velocity. In this context, the intraband section can be expressed as

$$\sigma=\sigma_{\text{intra}}=e^2\mu_c\tau/\left[\pi\hbar^2(1+j\omega\tau)\right], \quad (3)$$

for $\tau = 1/(2\Gamma) = \mu\hbar(n_s\pi)^{1/2}/(ev_F)$ the scattering time, μ the carrier mobility, and $n_s = (\mu_c)^2/[\pi(\hbar v_F)^2]$ the carrier density from (2).

III. Modified FDTD Method for Graphene Layers

The extraction of the proposed FDTD update equations is conducted through the implementation of Maxwell's integral equations and their subsequent discretization by a second-order accurate scheme in a modified $\Delta x\times\Delta y\times\Delta z$ Yee cell. Firstly, it should be clarified that for the rest of the domain, the conventional FDTD formulas are used, whereas the new change is required only at cells where the graphene sheet lies. Such a cell is depicted in Fig. 1(a), from which one may observe that the graphene surface conductivity is located at the center of the element at the xy-plane. In order to deal with the general case, the dielectric space above the graphene layer has a permittivity ε_1 and the one below the sheet a permittivity ε_2. On the surface conductivity, the surface current is given, in the frequency domain, by

$$\dot{\mathbf{J}}=\sigma\dot{\mathbf{E}}\,, \quad (4)$$

where σ is determined through (3) for $J_z = 0$. Note that the dot signifies components in the frequency domain.

Since graphene affects only the surface current term, the equations to be altered are only the ones derived from Ampere's

law, while those of the magnetic field remain the same. Additionally, the graphene surface current is expressed as

$$\mathbf{J}_{gr} = \mathbf{J}\delta(z), \tag{5}$$

with graphene located on the *xOy* plane. So, for instance, Ampere's integral law on the *xz*-plane of a modified Yee cell with the direct incorporation of (5) gives the E_y update equation, i.e.

$$\oint_C \mathbf{H}\cdot\mathbf{dl} = \iint_S \varepsilon\frac{\partial\mathbf{E}}{\partial t}\cdot\mathbf{dS} + \iint_S \mathbf{J}_{gr}\cdot\mathbf{dS} \Rightarrow E_y\Big|_{i+1/2,j+1/2,k}^{n+1}$$

$$= E_y\Big|_{i+1/2,j+1/2,k}^{n} + \frac{2\Delta t}{\varepsilon_1+\varepsilon_2}\left[\frac{1}{\Delta x}\left(H_z\Big|_{i-1,j+1/2,k}^{n+1/2} - H_z\Big|_{i+1,j+1/2,k}^{n+1/2}\right)\right.$$

$$\left. + \frac{1}{\Delta z}\left(H_x\Big|_{i,j,k+1/2}^{n+1/2} - H_x\Big|_{i,j,k-1/2}^{n+1/2}\right)\right] - \frac{2\Delta t}{(\varepsilon_1+\varepsilon_2)\Delta z}J_y\Big|_{i+1/2,j+1/2,k}^{n+1/2} \tag{6}$$

where the typical FDTD notation is supposed. The presence of Δz in the denominator of the last term means that J_y becomes the surface current density instead of the volume one in [8].

Owing to its frequency-dependent nature, the surface current term needs to be treated by an ADE scheme, in which (4) serves as the auxiliary equation. In this sense, (3) is written as

$$\sigma = \sigma_{\text{intra}} = A/(1+j\omega\tau), \tag{7}$$

with $A = e^2\mu_c\tau/(\pi\hbar^2)$ and so the auxiliary equation becomes

$$\dot{\mathbf{J}} = \sigma\dot{\mathbf{E}} \rightarrow \dot{J}_y = \sigma\dot{E}_y \Rightarrow \dot{J}_y = A\dot{E}_y/(1+j\omega\tau), \tag{8}$$

while in the time-domain it is written as

$$J_y\Big|_{i,j,k}^{n+3/2} = \frac{2\tau-\Delta t}{2\tau+\Delta t}J_y\Big|_{i,j,k}^{n+1/2} + \frac{2A\Delta t}{2\tau+\Delta t}E_y\Big|_{i,j,k}^{n+1}. \tag{9}$$

Similar equations hold for the E_x component, as well. In contrast, the E_z component is computed by a regular FDTD equation, as it does not lie on the surface of graphene.

IV. Numerical Results – Conclusions

For the validation of the new technique, we examine an infinite graphene sheet placed between two dielectric subspaces and illuminated by a set of normally incident wideband plane wave pulses. Based on the configuration of Fig. 1(b), the infinite dimensions of the structure are modeled through the imposition of periodic boundary conditions at the lateral surfaces of the domain, thus forming a computational unit cell. Moreover, the incident field is launched via a total-field scattered-field formulation [6], while the lattice comprises cubic cells with a spatial increment equal to the 1/20th of the minimum excited wavelength in the material with the highest relative permittivity. Particularly, the excitation follows a simple Gaussian rule in time, with a bandwidth of 2 GHz and a time-step set at the highest value allowed by the Courant limit. Note that at the upper and lower boundaries, an 8-cell perfectly matched layer (PML) is imposed.

The basic aim of the application is the extraction of the transmission coefficient. Consequently, the field at the second dielectric is monitored and its Fourier transform is extracted with an FFT scheme. As the normally incident electric field is linearly polarized along the *y*-axis, only one of its components is nonzero. So, for the extraction of the transmission coefficient, relation

$$T_t = F\{E_{trans}\}/F\{E_{inc}\}, \tag{10}$$

is applied, where E_{inc} is the time waveform of the incident field, E_{trans} that of the transmitted field, and $F\{.\}$ the Fourier transform operator. Two simulations are conducted in which $\mu_c = 0.3$ eV and $T = 300$ K. The scattering rate is $\Gamma = 0.11$ meV and corresponds to a mobility $\mu = 99729$ cm^2/Vs. Figure 2 illustrates the magnitude and Fig. 3 the phase of the transmission coefficient, as compared to the closed-form solution of the problem [7] and the outcomes of [8], where the graphene conductivity is modeled by a subcell technique. As observed, the three curves of each case are in a very good agreement; a fact that proves the accuracy and convergence of the proposed method, yet with a much simpler and faster realization. These deductions enable its application to finite-sized structures, which do not have an analytical solution and will be elaborately explored in the full paper.

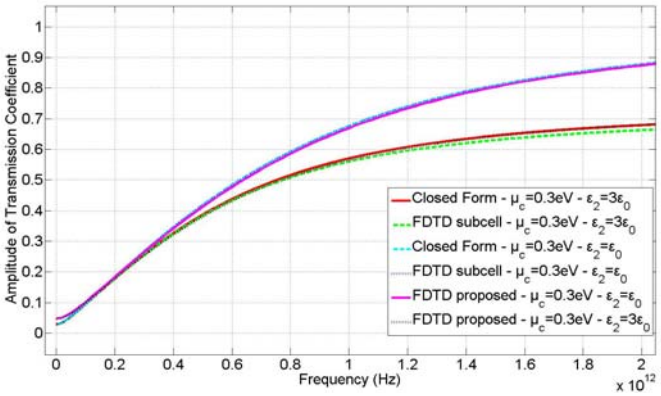

Fig. 2. Magnitude of the graphene transmission coefficient.

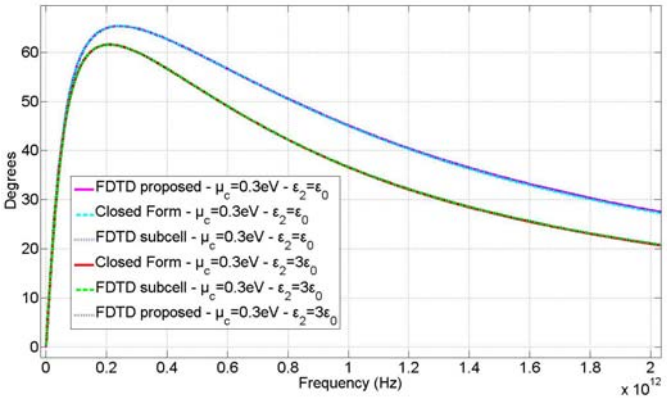

Fig. 3. Phase (in degrees) of the graphene transmission coefficient.

References

[1] E. W. Hill, A. K. Geim, K. Novoselov, F. Schedin, and P. Blake, "Graphene spin valve devices," *IEEE Trans. Magn.*, vol. 42, no. 10, pp. 2694–2696, Oct. 2006.

[2] V. P. Gusynin, S. G. Sharapov, and J. P. Carbotte, "Magneto-optical conductivity in graphene," *J. Phys.: Condens. Matter*, vol. 19, pp. 026222(1–25), 2007.

[3] T. Hiraiwa, R. Sato, A. Yamamura, J. Inoue, S. Honda, and H. Itoh, "Effects of magnetoresistance in FM/Graphene/FM lateral junctions," *IEEE Trans. Magn.*, vol. 47, no. 10, pp. 2743–2745, Oct. 2011.

[4] V. Panchal, D. Cox, R. Yakimova, and O. Kazakova, "Epitaxial graphene sensors for detection of small magnetic momdents," *IEEE Trans. Magn.*, vol. 49, no. 1, pp. 97–100, Jan. 2013.

[5] J. Chen, M. Badioli, A. González *et al.*, "Optical nano-imaging of gate-tuneable graphene plasmons," *Nature*, vol. 487, pp. 77–81, 2012.

[6] A. Taflove and S. C. Hagness, *Computational Electrodynamics: The Finite-Difference Time-Domain Method*. Norwood, MA: Artech House, 2005.

[7] G. Hanson, "Dyadic Green's functions and guided surface waves for a surface conductivity model of graphene," *J. Appl. Phys.*, vol. 103, art. no. 064302, 2008.

[8] G. Bouzianas, N. Kantartzis, C. Antonopoulos, and T. Tsiboukis, "Optimal modeling of infinite graphene sheets via a class of generalized FDTD schemes," *IEEE Trans. Magn.*, vol. 48, no. 2, pp. 379–382, Feb. 2012.